

Synchronous PWM Control of Triple Transformer-Connected Inverters for Photovoltaic System

V. Oleschuk¹, M. Cernat², M. Pastor³, P. Sanjeevikumar⁴

¹Academy of Sciences of Moldova, Chisinau, Republic of Moldova, ²Transilvania University, Brasov, Romania, ³Technical University of Kosice, Slovak Republic, ⁴University of Johannesburg, Auckland Park, South Africa
E-mail: oleschukv@hotmail.com, m.cernat@unitbv.ro, marek.pastor@tuke.sk, sanjeevi_12@yahoo.co.in

Abstract-This paper presents results of research of modulation processes in power conversion system with triple voltage source inverters, supplied by photovoltaic (PV) strings, and connected to a four-winding transformer. The transformer has in this case specific connections between the secondary windings and inverters, allowing providing of multilevel voltages at secondary windings of the transformer. Specialized space-vector-based strategy of pulsewidth modulation (PWM) has been used for control of inverters, insuring quarter-wave symmetry of winding voltages for any modulation indices and switching frequency of inverters. Analysis and comparison of harmonic composition of winding voltages and output voltages of inverters has been done. The validity of the analyzed processes has been verified by simulations: three basic variants of the scheme of modulation have been applied for control of inverters.

I. INTRODUCTION

Development of photovoltaic-focused power conversion systems is growing rapidly. Novel transformer-less and transformer-based topologies and configurations of solar photovoltaic installations for solar farms and solar factories have been proposed and investigated [1]-[4].

Recently, modified structure of transformer-based system with triple three-phase voltage source inverters has been proposed [5],[6]. Fig. 1 shows topology of this system for the case of delta-connection of secondary windings, supplied by three insulated strings of photovoltaic panels. Fig. 2 presents the corresponding secondary windings for the case of star-connection [6]. It has been shown in [6], that simple modification of connection between outputs of standard two-level inverters and windings of the transformer allow providing multilevel winding voltages for systems with insulated dc-sources. Also, winding voltages can be expressed in this case by the phase voltages of triple inverters.

Operation of inverter-based photovoltaic systems is in dependence of the used methods and techniques of PWM. Space-vector modulation is perspective method for control of inverters, including PV application. During system operation, for some regimes of photovoltaic systems (grid frequency fluctuation, different voltages of strings of PV panels, etc.) it is necessary to ensure voltage synchronization. So, this paper presents results of research of modulation processes in PV system with triple transformer-connected inverters, controlled by specialized schemes and techniques of space-vector PWM, insuring voltage synchronization and voltage symmetries for any operating conditions of the system.

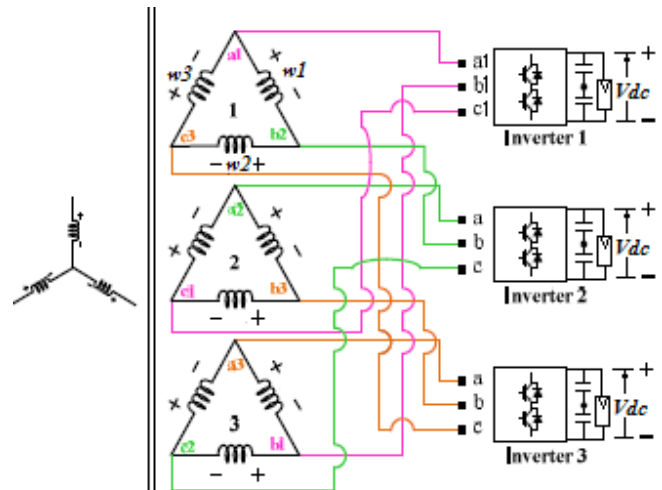


Fig. 1. Topology of transformer-based photovoltaic system with triple inverters specifically connected to secondary windings of the transformer (case of delta-connection of windings).

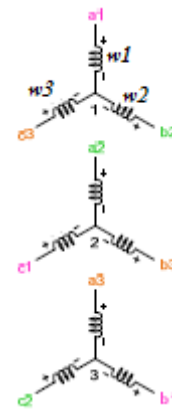


Fig. 2. Secondary windings of transformer of the system for the case of star-connection.

II. TWO-LEVEL INVERTERS WITH SYNCHRONOUS PWM

To assure voltage synchronization and waveform symmetries of inverters, specialized method of space-vector modulation can be used for control of triple inverters of PV system. Table I presents peculiarities and the main control dependences of this method of synchronous modulation, which are compared here with the corresponding parameters of conventional space-vector PWM [7]-[9].

TABLE I. BASIC PARAMETERS OF PWM METHODS

Control (modulation) parameter	Conventional schemes of space-vector PWM	Specialized method of modulation	
Operating and max parameter	Operating & max voltage V and V_m	Operating & maximum fundamental frequency F and F_m	
Modulation index m	V/V_m	F/F_m	
Duration of sub-cycles	T	τ	
Center of the k -signal	α_k (angles/degr.)	$\tau(k-1)$ (sec)	
Switch-on durations	$T_{ak} = 1.1mT[\sin(60^\circ - \alpha_k) + \sin \alpha_k]$ $t_{ak} = 1.1mT \sin \alpha_k$ $t_{bk} = 1.1mT \times \sin(60^\circ - \alpha_k)$	Algebraic PWM	Trigonometric PWM
		$\beta_k = \beta_1[1 - A \times (k-1)\pi FK_{ov1}]$	$\beta_k = \beta_1 \times \cos[(k-1)\pi K_{ov1}]$
		$\gamma_k = \beta_{i-k+1}[0.5 - 6(i-k)\pi F]K_{ov2}$	$\gamma_k = \beta_{i-k+1}[0.5 - 0.9\pi(i-k)\tau]K_{ov2}$
		$\beta_k - \gamma_k$	$\beta_k - \gamma_k$
Switch-off states (zero voltage)	$t_{0k} = T - t_{ak} - t_{bk}$	$\lambda_k = \tau - \beta_k$	
Special parameters providing synchronization of the process of PWM		$\beta'' = \beta_1[1 - A \times (k-1)\pi FK_{ov1}]K_s$	$\beta'' = \beta_1 \times \cos[(k-1)\pi K_{ov1}]K_s$
		$\lambda' = (\tau - \beta'') \times K_{ov1}K_s$	$\lambda' = (\tau - \beta'') \times K_{ov1}K_s$

III. SYNCHRONOUS PWM OF INVERTERS IN TRIPLE-INVERTER-BASED SYSTEM

Phase voltages V_{as1} , V_{bs1} and V_{cs1} of the first standard three-phase inverter (**Inverter 1** in Fig. 1) of the system are calculated in accordance with (1)-(3) [7]:

$$V_{as1} = V_{a10} + (V_{a10} + V_{b10} + V_{c10})/3 \quad (1)$$

$$V_{bs1} = V_{b10} + (V_{a10} + V_{b10} + V_{c10})/3 \quad (2)$$

$$V_{cs1} = V_{c10} + (V_{a10} + V_{b10} + V_{c10})/3, \quad (3)$$

where V_{a10} , V_{b10} and V_{c10} are the corresponding pole voltages of the first inverter.

Winding voltages of secondary windings of the system (V_{w1} , V_{w2} , V_{w3} in Fig. 1) can be expressed by the phase voltages of triple inverters in accordance with (4)-(9) [6]. Dependences (4)-(6) correspond to the case of delta-connection of windings, presented in Fig. 1, dependences (7)-(9) correspond to the case of star-connection, presented in Fig. 2.

$$V_{w1} = V_{as3} - V_{bs1} \quad (4)$$

$$V_{w2} = V_{bs1} - V_{cs2} \quad (5)$$

$$V_{w3} = V_{cs2} - V_{as3} \quad (6)$$

$$V_{w1} = 0.667V_{as1} - 0.333V_{bs2} - 0.333V_{cs3} \quad (7)$$

$$V_{w2} = -0.333V_{as1} + 0.667V_{bs2} - 0.333V_{cs3} \quad (8)$$

$$V_{w3} = -0.333V_{as1} - 0.333V_{bs2} + 0.667V_{cs3} \quad (9)$$

Control and output signals of triple inverters of the system are shifted by 120° (120° interleaving in accordance with some definitions). Also, small additional shift between control signals of three inverters, equal to $1/3$ of duration of the switching period (switching sub-cycle) has been provided by the used scheme of control and modulation.

Figs. 3 – Fig. 13 present results of simulation of processes in the system on the base of triple synchronously modulated inverters, and show basic voltage waveforms (pole voltages V_{a10} , V_{b10} , V_{c10} of the first inverter, phase V_{as1} and line-to-line V_{a1b1} voltages of the first inverter, and also winding voltages $V_{w1phase}$ and V_{w1line} , corresponding to the cases of star-connection and delta-connection of windings). It present also spectra of the phase V_{as1} and line V_{a1b1} voltages of inverters, and also spectra of winding voltages $V_{w1phase}$ and V_{w1line} .

Figs. 3-4 show voltage waveforms and voltage spectra of the system controlled in accordance with scheme of continuous synchronous modulation [7]. The fundamental frequency of the system is equal to $F=50\text{Hz}$, and switching frequency is equal to $F_s=1.13\text{kHz}$. Modulation index is equal to $m=0.65$ in this case.

Figs. 5-7 present voltage waveforms and the corresponding voltage spectra of system controlled by the scheme of synchronous discontinuous space-vector PWM with the 30° -non-switching intervals ([7], DPWM30, $F=50\text{Hz}$, average $F_s=1.13\text{kHz}$, $m=0.75$).

Figs. 8-9 illustrate modulation processes in system controlled by scheme of synchronous discontinuous space-vector PWM with the 60° -non-switching intervals ([7], DPWM60, $F=50\text{Hz}$, average $F_s=1.13\text{kHz}$, $m=0.85$).

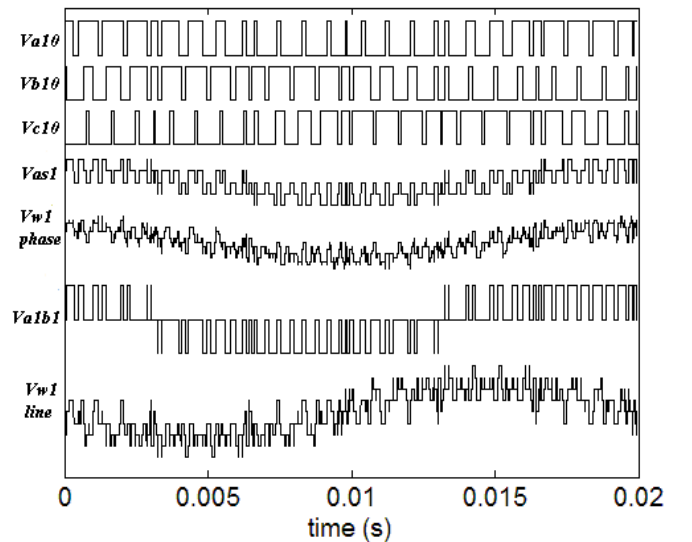


Fig. 3. Pole voltages V_{a10} , V_{b10} , V_{c10} , phase voltage V_{as1} , line voltage V_{a1b1} of the first inverter, and the corresponding winding voltages $V_{w1phase}$ and V_{w1line} of the system with continuous synchronous PWM (CPWM, $F=50\text{Hz}$, $F_s=1.13\text{kHz}$, $F_s/F=24.6$, $m=0.65$).

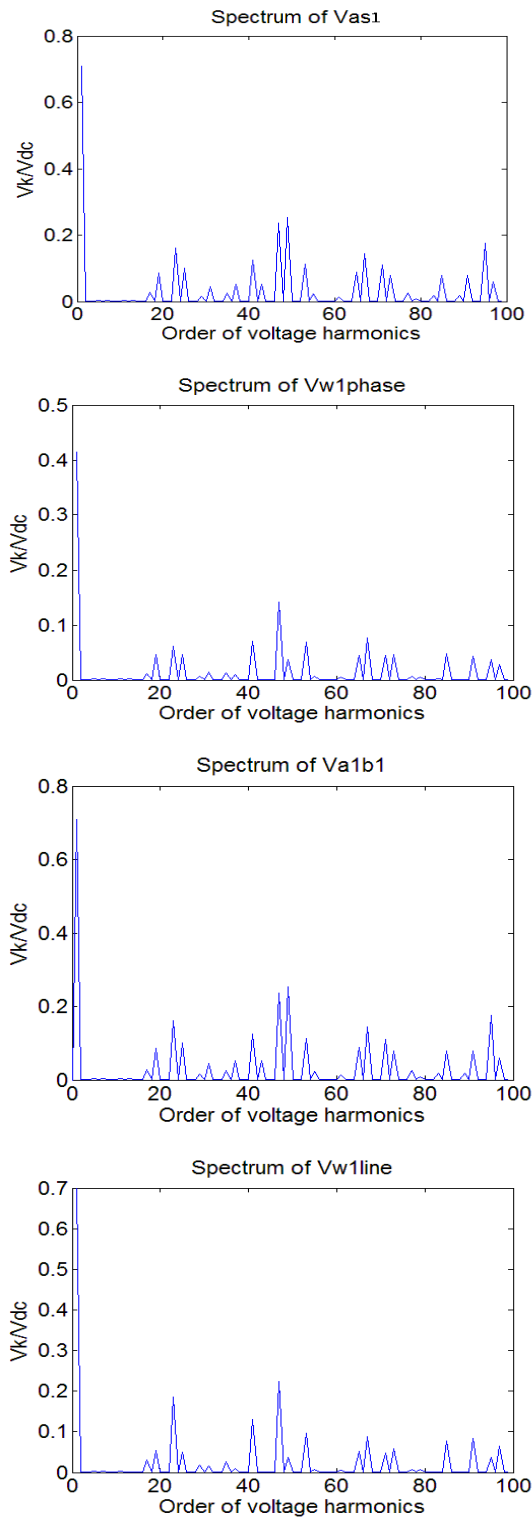


Fig. 4. Spectra of voltage waveforms of the system with continuous synchronous PWM ($F=50\text{Hz}$, $F_s=1.13\text{kHz}$, $m=0.65$).

Figs. 10-13 illustrate regimes of operation of inverters with discontinuous PWM in two parts of the zone of overmodulation (Figs. 10-11: the first part of the zone of modulation – DPWM60, $F=50\text{Hz}$, average $F_s=1.13\text{kHz}$, $m=0.95$; Figs. 12-13: the second part of the overmodulation zone – DPWM30, $F=50\text{Hz}$, average $F_s=1.13\text{kHz}$, $m=0.975$).

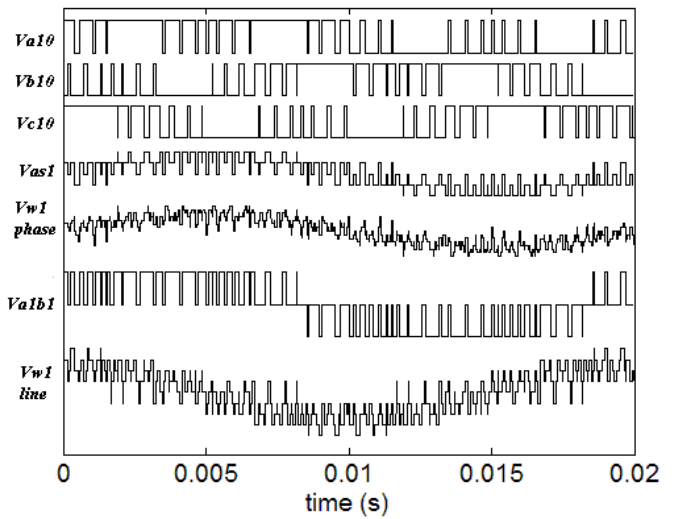


Fig. 5. Pole voltages V_{a10} , V_{b10} , V_{c10} , phase voltage V_{as1} , line voltage V_{a1b1} of the first inverter, and the corresponding winding voltages $V_{w1\text{phase}}$ and $V_{w1\text{line}}$ of the system with discontinuous synchronous PWM (DPWM30, $F=50\text{Hz}$, $F_s=1.13\text{kHz}$, $F_s/F=24.6$, $m=0.75$).

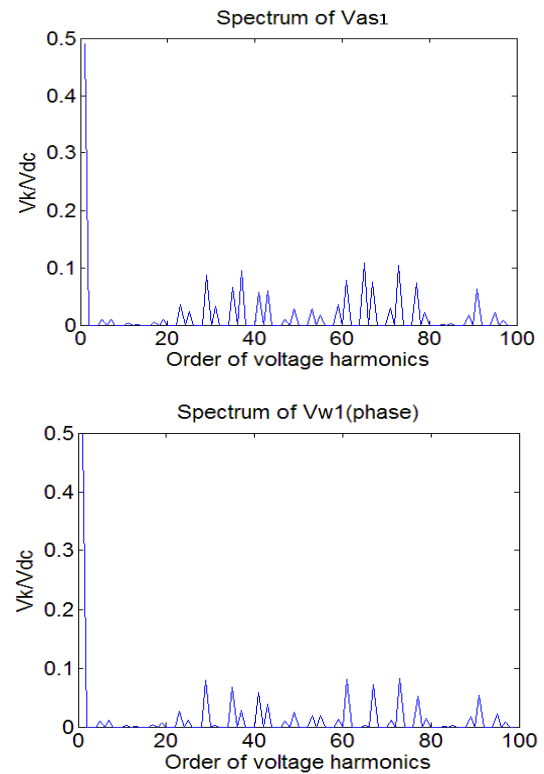


Fig. 6. Spectra of voltage waveforms of the system with discontinuous PWM (DPWM30, $F=50\text{Hz}$, $F_s=1.13\text{kHz}$, $m=0.75$).

To emphasize properties of the used specialized scheme of PWM, fractional frequency ratio between the switching and fundamental frequencies (equal to $1130\text{Hz}/50\text{Hz}=22.6$) has been used. Analysis of harmonic composition of symmetrical (with quarter-wave symmetry) voltage waveforms of the system shows (see Figs. 6, 7, 9, 11, 13), that spectra of the all presented waveforms do not include even harmonics and subharmonics for any values of modulation indices of inverters operating at both linear and overmodulation zones.

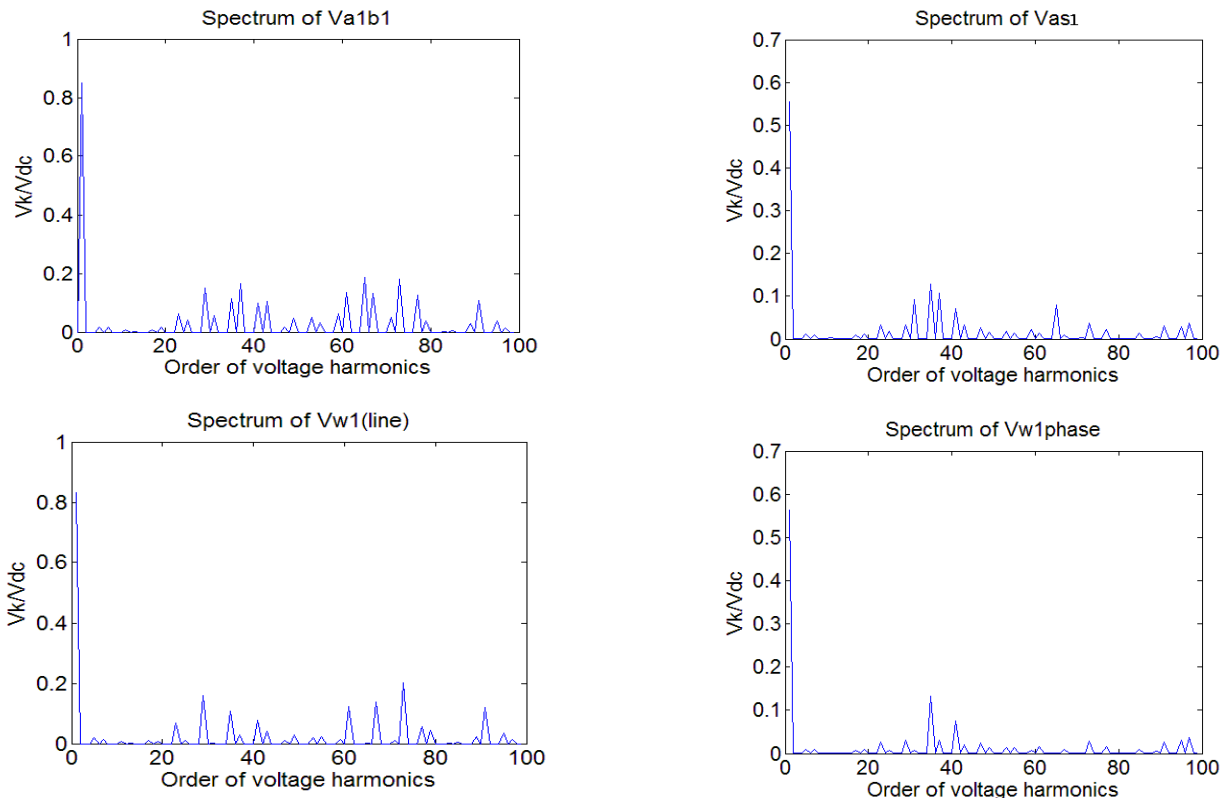


Fig. 7. Spectra of voltage waveforms of the system with discontinuous PWM (DPWM30, $F=50\text{Hz}$, $F_s=1.13\text{kHz}$, $m=0.75$).

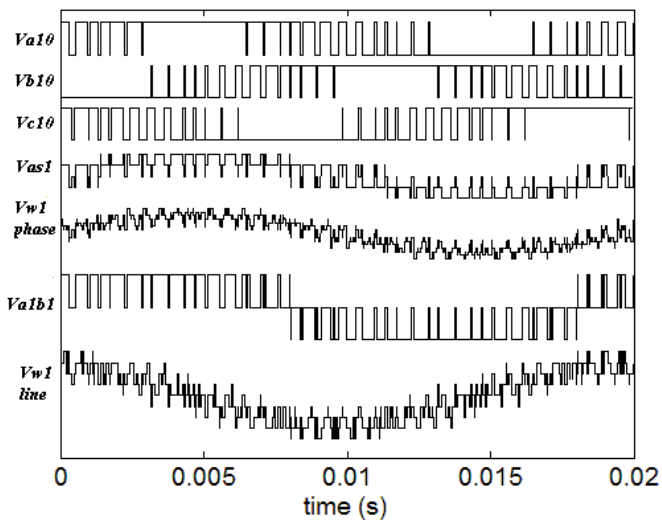


Fig. 8. Pole voltages $V_{a1\theta}$, $V_{b1\theta}$, $V_{c1\theta}$, phase voltage V_{as1} , line voltage V_{a1b1} of the first inverter, and the corresponding winding voltages $V_{w1\text{phase}}$ and $V_{w1\text{line}}$ of the system with discontinuous synchronous PWM (DPWM60, $F=50\text{Hz}$, $F_s=1.13\text{kHz}$, $F_s/F=24.6$, $m=0.85$).

Total Harmonic Distortion factor is an important criterion for analysis and comparison of voltage waveforms in photovoltaic systems. In particular, for 50-Hz systems it has been recommended to take into consideration harmonics up to the 40th voltage harmonic for determination of total voltage harmonic distortion factor [10]. Figs. 14-15-present results of calculation of Total Harmonic Distortion factor (*THD*) for basic voltage waveforms of the system as function of

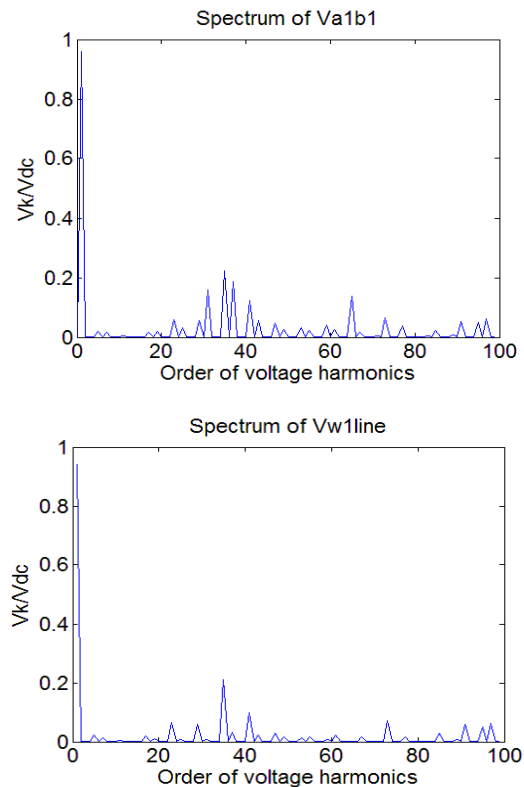


Fig. 9. Spectra of voltage waveforms of the system with discontinuous PWM (DPWM60, $F=50\text{Hz}$, $F_s=1.13\text{kHz}$, $m=0.85$).

modulation index m of triple inverters, controlled by synchronous techniques of continuous (CPWM) and discontinuous (DPWM30 and DPWM60) pulsewidth modulation.

THD factor has been calculated until the 40-th low-order (k -th) voltage harmonic (Fig. 14, $THD = (1/V_{w1_1}) \sqrt{\sum_{k=2}^{40} V_{w1_k}^2}$), and also until the 1000-th harmonic (Fig. 15, $THD = (1/V_{w1_1}) \sqrt{\sum_{k=2}^{1000} V_{w1_k}^2}$). The fundamental frequency of the system was equal to 50Hz, and the average switching frequency of triple inverters was equal to 1.4kHz.

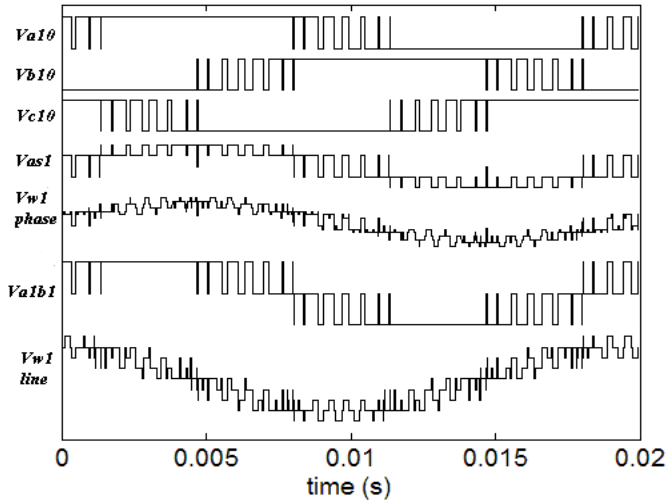


Fig. 10. Pole voltages V_{a10} , V_{b10} , V_{c10} , phase voltage V_{as1} , line voltage V_{a1b1} of the first inverter, and the corresponding winding voltages $V_{w1phase}$ and V_{w1line} of the system with discontinuous synchronous PWM in the overmodulation zone (DPWM60, $F=50\text{Hz}$, $F_s=1.13\text{kHz}$, $F_s/F=24.6$, $m=0.95$).

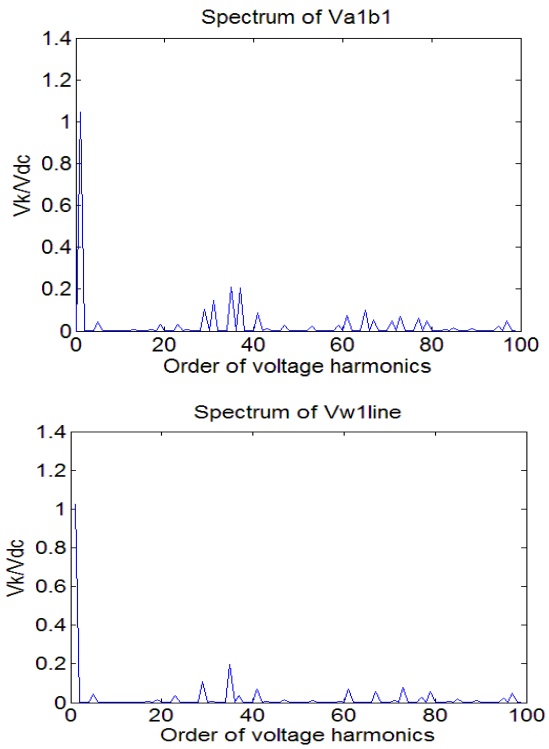


Fig. 11. Spectra of voltage waveforms of the system with discontinuous PWM (DPWM30, $F=50\text{Hz}$, $F_s=1.13\text{kHz}$, $m=0.95$).

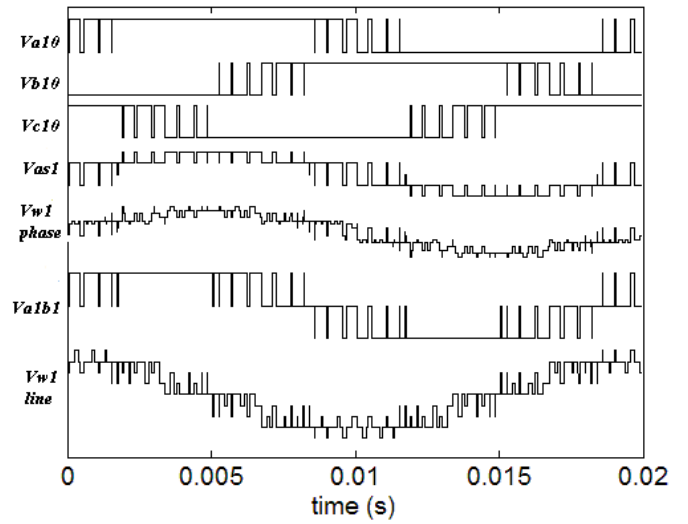


Fig. 12. Pole voltages V_{a10} , V_{b10} , V_{c10} , phase voltage V_{as1} , line voltage V_{a1b1} of the first inverter, and the corresponding winding voltages $V_{w1phase}$ and V_{w1line} of the system with discontinuous synchronous PWM in the overmodulation zone (DPWM30, $F=50\text{Hz}$, $F_s=1.13\text{kHz}$, $F_s/F=24.6$, $m=0.975$).

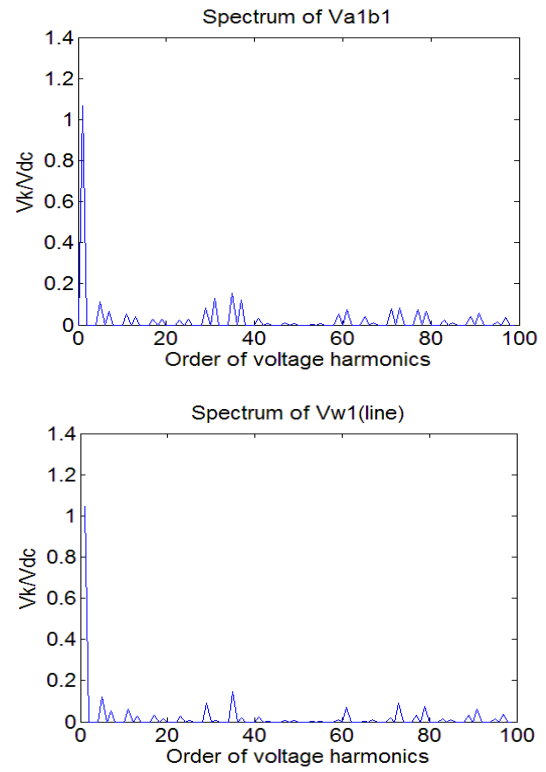


Fig. 13. Spectra of voltage waveforms of the system with discontinuous synchronous PWM (DPWM30, $F=50\text{Hz}$, $F_s=1.13\text{kHz}$, $m=0.975$).

Analysis of the presented in Fig. 14 and Fig. 15 results of calculation of THD factor shows, that due to the proposed in [6] connection between triple inverters and the secondary windings of the transformer, there is appreciable improvement of integral spectral characteristics of winding voltages. As an example, in accordance with diagram of Fig. 14 (for the case, if $m=0.7$), THD factor for winding voltages is reduced by 14% (for system with algorithm of CPWM), by 8% (for system controlled by algorithm of DPWM30), and

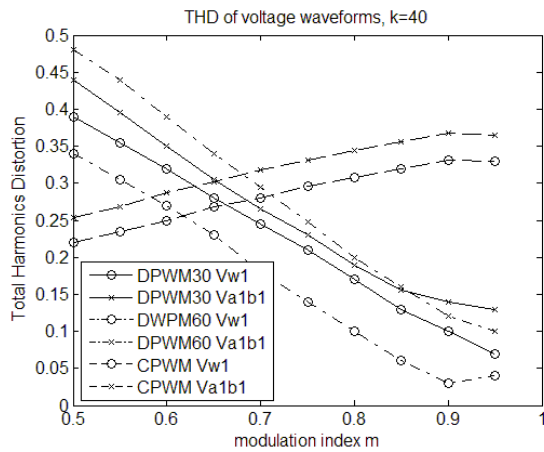


Fig. 14. *THD* factor of voltages of the system versus modulation index m ($k=40$).

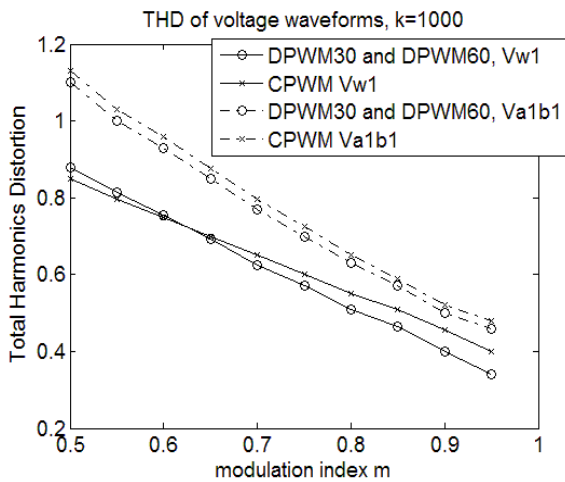


Fig. 15. *THD* factor of voltages of the system versus modulation index m ($k=1000$).

by 63% for system with DPWM60, in comparison with the corresponding line voltages. Accordingly, data of the diagram, presented in Fig. 15, show (as an example, for the case, if $m=0.7$), that *THD* factor for winding voltages of system with new connection between inverters and transformer is decreased by 23% (for system with DPWM30 or DPWM60), and by 22% (for system controlled by algorithm of CPWM), in comparison with the corresponding line voltages (case of conventional connection between inverters and transformer).

So, improved spectral composition of winding voltages of transformer-based system assures to reduce copper loss in windings of the transformer, and also to decrease switching and conduction losses at triple inverters.

IV. CONCLUSION

Specialized schemes and techniques of feedforward space-vector modulation, insuring voltage synchronization and voltage symmetries of inverters, can be used effectively in transformer-based photovoltaic systems on the base of triple inverters with novel connection between inverters and

windings of the transformer.

The presented voltage spectrograms illustrate qualitatively and quantitatively attenuation of the corresponding harmonics of winding voltages due to new connections inside the system.

To emphasize properties of the used specialized scheme of PWM, fractional frequency ratio between the switching frequency and fundamental frequency (equal to $1130\text{Hz}/50\text{Hz}=22.6$) has been chosen for analysis of modulation processes in system. Research of harmonic composition of symmetrical (with quarter-wave symmetry) voltage waveforms of the system shows (see Figs. 6, 7, 9, 11, 13), that spectra of the all presented waveforms do not include even harmonics and subharmonics for any values of modulation indices of inverters operating at both linear control zone and zone of overmodulation..

It has been shown, that in general case *THD* factor for winding voltages of secondary windings of the system with new connection between inverters and transformer is decreased (in average) by about 20% for systems with both continuous and discontinuous synchronous PWM, in comparison with the case of conventional connection between inverters and transformer.

ACKNOWLEDGMENT

This work was supported by the Slovak Research and Development Agency under the contract no. APVV-15-0750 and by the project no. FEI-2015-3.

REFERENCES

- [1] G. Grandi, C. Rossi, D. Ostojic, and D. Casadei, "A new multilevel conversion structure for grid-connected PV applications," *IEEE Trans. Ind. Electron.*, vol. 56, no. 11, pp. 4416–4426, 2009.
- [2] G. Spagnuolo, et al., "Renewable Energy Operation and Conversion Schemes", *IEEE Ind. Electr. Magazine*, vol. 4, no. 1, pp. 38-51, 2010.
- [3] V. Oleschuk and G. Griva, "Simulation of processes in synchronized cascaded inverters for photovoltaic application," *International Review of Electrical Engineering*, vol. 4, no. 5, pp. 975-982, 2009.
- [4] *Renewable Energy, Selected Issues*, vol. 2. Cambridge Scholars Publishing, pp. 166-247, 2016.
- [5] Yongsoo Park, Sungjae Ohn, and Seung-Ki Sul, "Multi-level operation with two-level converters through a double-delta source connected transformer," *Journal of Power Electronics*, vol. 14, no. 6, pp. 1093-1099, 2014.
- [6] Sungjae Ohn, Yongsoo Park, and Seung-Ki Sul, "Multi-level operation of triple two-level PWM converters," *Proc. of IEEE Energy Conversion Congress and Exposition (ECCE'2015)*, pp. 4283-4289, 2015.
- [7] F. Blaabjerg, V. Oleschuk, and F. Lungeanu, "Synchronization of output voltage waveforms in three-phase inverters for induction motor drives," *Proc. of IEEE-IEEJ Power Conversion Conf. (PCC'2002)*, pp. 528-533, 2002.
- [8] V. Oleschuk, G. Grandi, and P. Sanjeevikumar, "Simulation of processes in dual three-phase system on the base of four inverters with synchronized modulation," *Advances in Power Electronics*, vol. 2011, pp. 1-9, 2011.
- [9] V. Oleschuk and F. Barrero, "Standard and non-standard approaches for voltage synchronization of drive inverters with space-vector PWM: A survey," *International Review of Electrical Engineering*, vol. 9, no. 4, pp. 688-707, 2014.
- [10] M. Aiello, A. Cataliotti, S. Favuzza, and G. Graditi, "Theoretical and experimental comparison of Total Harmonic Distortion factors for the evaluation of harmonic and interharmonic pollution of grid-connected photovoltaic systems," *IEEE Trans. Power Delivery*, vol. 21, no. 3, pp. 1390-1397, 2006.